Journal of Sedimentary Research

Journal of Sedimentary Research, 2006, v. 76, 589–604
Research Article
DOI: 10.2110/jsr.2006.045

CORRELATION OF TERRESTRIAL CLIMATIC FLUCTUATIONS WITH GLOBAL SIGNALS DURING THE UPPER CRETACEOUS–DANIAN IN A COMPRESSIVE SETTING (PROVENCE, FRANCE)

ISABELLE COJAN[1] AND MARIE-GABRIELLE MOREAU[2]
[1]*Ecole Nationale Supérieure des Mines de Paris, CGES-Sédimentologie, 77305 Fontainebleau Cedex, France*
[2]*Institut Physique du Globe de Paris (IPGP), Laboratoire Paléomagnétisme, 75252 Paris*
e-mail: Isabelle.Cojan@ensmp.fr

ABSTRACT: **The Upper Cretaceous-lower Paleocene terrestrial formations from the Aix-en-Provence basin offer a high-resolution record of the effects of climate changes. These units were deposited in a basin with low topographic relief under climate conditions that varied from subhumid to semiarid. Sedimentation during subhumid periods was characterized by accumulation of carbonate mud in the main lake and aggradation of floodplains during overbank floods. Carbonate-rich paleosols, which occur throughout the subhumid succession, contain authigenic minerals with interstratified illite–smectite and smectite.**

Although subhumid conditions were dominant during deposition, the occurrence of five semiarid episodes can be documented on the basis of facies, paleomagnetic signal, and mineralogic associations of rocks deposited across the paleolandscape. The lake-margin environment was most sensitive to climate change. Dolomite and gypsum crystals, authigenic smectite and palygorskite, and secondary fine-grained hematite grew within rocks deposited along the lake margin under semiarid conditions. The mineralogic transformations resulted in a distinct paleomagnetic record composed of a lt component (200 to 400°C) and an associated chemo-detrital ht component (up to 600°C). During the semiarid episodes, sedimentation in floodplain environments was reduced, allowing development of mature smectite or smectite–palygorskite paleosols.

Semiarid episode 1 occurs within the Calcaire de Rognac Formation, semiarid episodes 2 and 3 lie within the Upper Argiles Rutilantes Formation, and semiarid episodes 4 and 5 are just below and within the Calcaire de Vitrolles Formation. Recognition of correlative deposits with a distinct paleomagnetic signal allows correlation between the continental successions of Provence and the geomagnetic polarity time scale. The lithostratigraphic units, as well as the distribution of dinosaur oospecies are largely diachronous, representing a few millions of years.

Semiarid episodes 1 to 3 occurred during the Early Maastrichtian. No semiarid episodes are recorded for the cooler interval that defined the Middle–Late Maastrichtian. Semiarid episodes 4 and 5 correspond to the warmer periods that preceded and followed the 500-ky-long interval containing the Cretaceous–Tertiary boundary.

INTRODUCTION

Understanding the relative importance of tectonic and climatic controls on continental sedimentation is important for interpreting the resulting architecture of stratigraphic units. Several models have been proposed to explain the effects of changes in sediment supply, subsidence rate, and base level (Posamentier and Allen 1993; Leeder et al. 1998; Carroll and Bohacs 1999). Although some consider climate to exert a major control on sedimentation (Cecil 1990; Heller and Paola 1992; Paola et al. 1992; Carroll and Bohacs 1999; Martinius 2000), others emphasize the importance of tectonics in foreland and extensional basins (De Celles 1986; Blair and Bilodeau 1988; Olsen 1990; Smith 1994; May et al. 1995; Diessel et al. 2000; Hoppie and Garrison 2002).

This paper presents a study of the Upper Cretaceous to Lower Paleocene continental successions of the Aix-en-Provence basin. These strata record the effects of climatic fluctuations. Sedimentologic, mineralogic, and paleomagnetic data collected make it possible to compare the regional signal from this continental succession with global climatic fluctuations.

GEOLOGICAL SETTING

The Aix-en-Provence basin is bounded on the north and south by reverse and thrust faults that have been active throughout late Cenozoic times (Durand and Guieu 1980) (Fig. 1A). Continental sedimentation in the Aix-en-Provence basin began in the Santonian and lasted for more than 30 My. During this period, no major paleogeographic rearrangement occurred in the basin, which continuously subsided due to Pyreneo-Provençal deformation (N–S compression) (Durand 1989; Westphal and Durand 1990). Upper Cretaceous to Lower Tertiary continental deposits are unconformably overlain by Miocene marine facies. The Upper Cretaceous to Lower Tertiary successions are composed of shallow lacustrine carbonates interbedded with alluvial and fluvial deposits that were derived from carbonate uplands located to the north and south and from the Maure Mountains located to the east (Gaviglio 1987).

The study area is located between the Berre Laguna on the west and the village of Puyloubier on the east (Fig. 1). The analyzed sections are exposed along north–south and east–west trending ridges. Lateral physical correlations were established where possible.

 1527-1404/06/076-589/$03.00

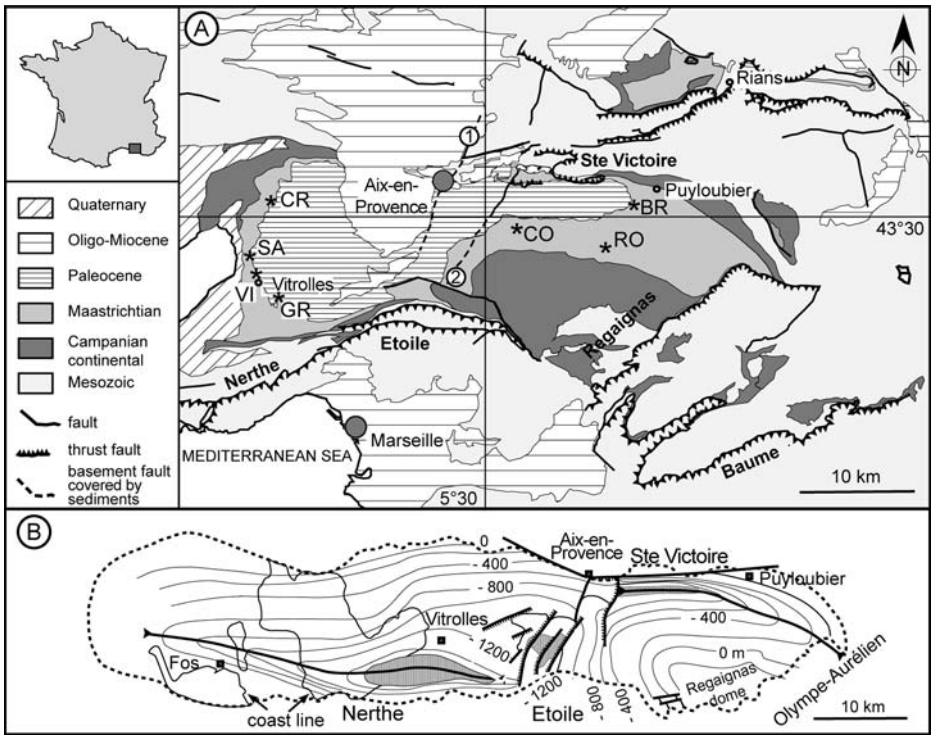

FIG. 1.—**A)** Location map and schematic geological map of the Aix-en-Provence basin (modified after the Carte Géologique Marseille, 1/250,000, Rouire et al. 1979). Measured sections: BR, Bréguières; CO, Collet Rouge; CR, Collet Redon; GR, Griffon; RO, Rousset; SA, Sarragousse; VI, Vitrolles Radar. 1, Aix-en-Provence fault; 2, Meyreuil fault. **B)** Present structural pattern of the Aix-en-Provence basin based on a structure contour map of the "Grande Mine" lignite that is close to the base of the Fuvelian (modified after Glintzboeckel 1980).

Structural Context

Along the northern border of the basin (Sainte Victoire Massif) the geometry of the two major thrust faults is considered to be inherited from paleofaults that were active during the Early Jurassic. These faults controlled the location of the boundary between the Provence platform and the Alpine basin (Dardeau 1987; Chorowitz et al. 1989). Reconstruction of paleostress orientations indicates several episodes of folding and strike-slip and reverse faulting that occurred during Late Cretaceous N–S compression (Lacombe et al. 1992). These deformations resulted in upwarping of the Regaignas dome and development of a radiating stress distribution along the southern edge of the basin (Etoile Massif); sinistral strike-slip displacements along the NE–SW oriented Aix-en-Provence and Meyreuil faults affected the basin as a whole (Gaviglio 1985).

Major shortening of the Provence sedimentary cover occurred during late Eocene NNE–SSW compression (Paris 1969). Displacements associated with strike-slip faults occurred during the Oligocene (Gaviglio 1987). Along the Meyreuil fault, dextral oblique movements occurred during the Miocene (Gaviglio 1985).

The present configuration of the Aix-en-Provence Basin is interpreted as the consequence of later compressional events (Durand and Guieu 1980). Post-Miocene structural evolution of the basin resulted in the development of two strongly asymmetric E–W-trending synclines separated by a N-trending fault system (Fig. 1B) (Glintzboeckel 1980; Gaviglio 1987).

Stratigraphy

Our study is focused on the late Campanian, Maastrichtian, and Danian continental successions of the Aix-en-Provence basin. These correspond to the Rognacian and Vitrollian continental stages as classically defined in the continental successions of southern France (Babinot and Durand 1980a, 1980b) (Fig. 2). This stratigraphic interval of interest consists of three formations: (1) the Calcaire de Rognac Formation (C. Rognac Fm), dominated by lacustrine carbonate facies; (2) the overlying Upper Argiles Rutilantes Formation (U. Argiles Fm),

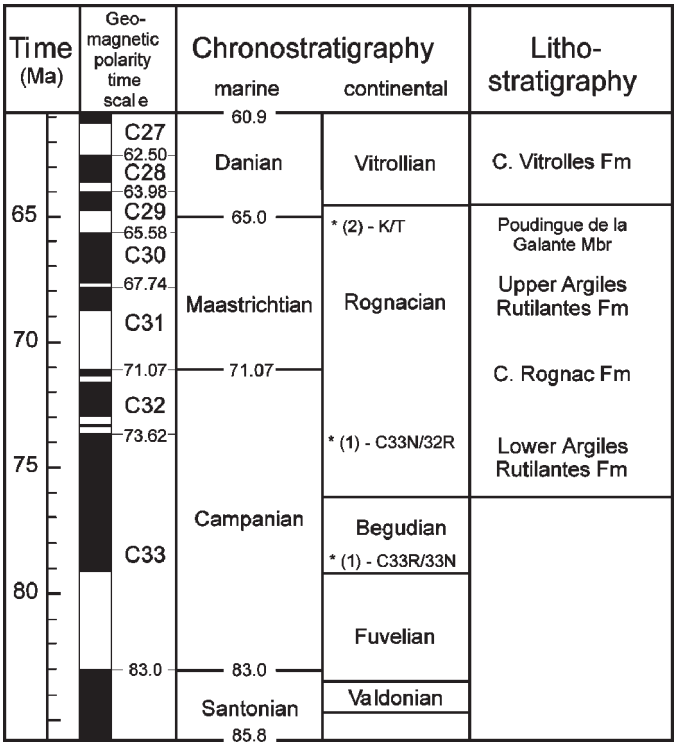

FIG. 2.—Chronostratigraphic and lithostratigraphic framework of the Upper Cretaceous–lower Tertiary continental succession from the Aix-en-Provence Basin. Time scale is from Cande and Kent (1995). Chronostratigraphy of the Provence continental stages, based on magnetostratigraphic correlations (1, Westphal and Durand 1990) combined with isotopic studies (2, Cojan et al. 2000) is indicated.

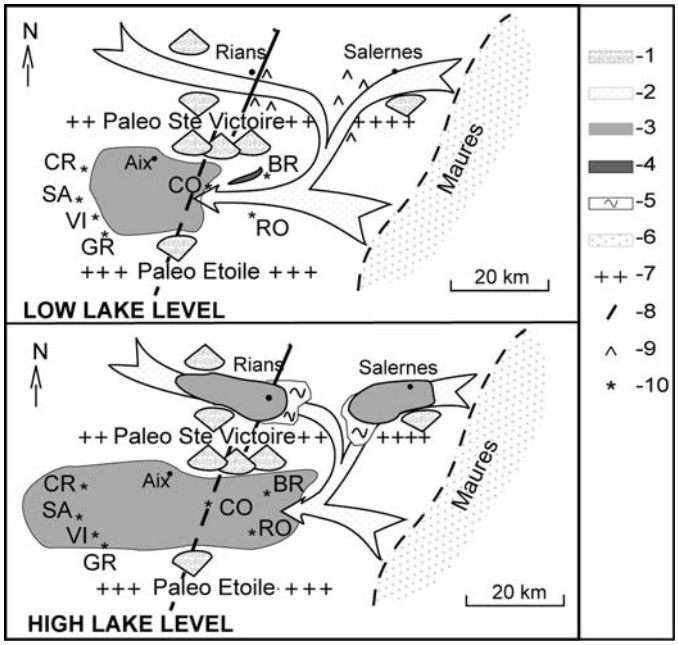

FIG. 3.—Schematic diagram showing changes in depositional environments associated with high and low lake levels. Highlands bordering the basin to the north and south are the paleo Sainte Victoire and the paleo Etoile, respectively. Legend: 1, proximal lateral alluvial fan; 2, main fluvial system; 3, lake extension; 4, playa facies; 5, reworked lacustrine material; 6, older substrate consisting of igneous rocks and Permian sandstones; 7, topographic high; 8, fault; 9, salt diapir; 10, studied sections.

ranging from palustrine to fluvial deposits; and (3) the Calcaire de Vitrolles Formation (C. Vitrolles Fm), characterized by shallow lacustrine carbonate facies. The C. Rognac Fm and the C. Vitrolles Fm can be traced laterally, but they undergo substantial lateral facies changes as well as changes in thickness (Cojan 1989; Colson 1996).

The distribution of fossils in these formations is closely related to the depositional facies. Upper Cretaceous strata are characterized by some charophytes in the C. Rognac Fm (Feist-Castel 1975). The base of the Paleogene is located within a 70-m-long interval defined by the last occurrence of dinosaur eggs (Westphal and Durand 1990) and the first Paleocene gastropod occurrence (Vasseur 1898). Paleomagnetic studies support and have refined this stratigraphic framework. The C. Rognac Fm was deposited during most of Chron 32 and the lower part of Chron 31R in the eastern part of the basin, but in the western part no precise paleomagnetic correlation has been proposed (Krumsiek and Hahn 1989; Westphal and Durand 1990). Capping the C. Rognac Fm, the Upper Argiles Fm extends up to the Cretaceous–Tertiary boundary. The Cretaceous–Tertiary boundary has been located a few meters below the C. Vitrolles Fm on the basis of combined magnetostratigraphy and chemostratigraphy (Cojan et al. 2000). The C. Vitrolles Fm spans most of the Danian (Cojan et al. 2000).

Paleogeography

During the Late Cretaceous–early Tertiary, the Aix-en-Provence basin was located at 35° N (Besse and Courtillot 2002; Dercourt et al. 2000). Deposition took place in a fluvial network that flowed into a shallow perennial lake (Cojan 1993) (Fig. 3). The fluvial system was characterized by a low-gradient floodplain inundated by lakes during high lake levels. Because there were no direct connections with sea, base level was controlled by the water level of a closed lake (Freytet and Plaziat 1982; Colson and Cojan 1996).

Stratigraphic successions are dominated by silty alluvium with minor braided-channel fills, distal alluvial-fan deposits, and lacustrine carbonates. Pedogenesis was extensive in alluvial facies and palustrine carbonates. Numerous carbonate-rich paleosols are present in the successions, but pseudogleys are fairly rare (Cojan 1999). The occurrence of carbonate-rich paleosols and the palynological record indicate that the climate was warm and markedly seasonal with rainfall below 400 mm/year (Medus 1972; Ashraf and Erben 1986; Duchaufour 2001) at the time of deposition.

METHODS

Seven sections, described at a 10-cm-scale, were studied in the Aix-en-Provence syncline (Fig. 1). Sampling for the different types of analysis (facies description, mineralogy, and magnetostratigraphy) was performed at the same time. Samples were collected as much as possible with a regular spacing from any facies.

Facies Description

Thin sections and polished slabs were prepared using standard methods to examine textures. Cathodoluminescence petrography was carried out on polished thin sections using a Technosyn 8200 Mk II luminoscope. The cold cathode gun was operated with a 350–420 mA beam current and a 15 kV gun potential.

Mineralogy

Bulk rock composition and clay mineralogy were determined by X-ray diffraction (XRD) analysis, using a Philips PW 1729 diffractometer with Cu-Kα radiation. Bulk rock analysis was performed on randomly oriented powdered samples. The clay mineralogy analysis was conducted on the < 2 μm size fraction, which was extracted from the whole-rock samples using conventional sedimentation techniques. The analytical procedure for clay-mineral identification is given in Thiry et al. (1983). The estimated error for both bulk rock and clay mineralogy is approximately $\pm$ 5%.

Magnetic Studies

Three sections were sampled for magnetostratigraphy (CR, 54 samples; VI, 70 samples; and BR, 38 samples). Samples were collected with a portable drill (2.5 cm diameter cores) and oriented with a sun and/or magnetic compass. Hand samples were collected from poorly consolidated lithologies, and cores were later drilled in the laboratory. The remanent magnetization of the samples was measured using a CTF cryogenic magnetometer in the shielded paleomagnetic laboratory of IPGP. The magnetic carriers were investigated by acquisition and thermal demagnetization of IRM (isothermal remanent magnetization), following the method described by Lowrie (1990). Magnetic fields of 1.2, 0.4, and 0.12 T (hard, medium, and soft components) were successively applied to each of the three perpendicular sample axes prior to thermal demagnetization.

Thermal and occasionally alternative field demagnetization techniques were used for NRM characterization (natural remanent magnetization). Characteristic remanent components were defined using principal-components analysis (Kirschvink 1980). When isolation of components failed and demagnetization paths seemed to fit a great circle, this was later calculated using the technique of McFadden and McElhinny (1988).

RESULTS

Facies and Depositional Environment

The continental successions are dominated by fine-grained limestone, shale, and siltstone facies. Sandstones and conglomerates are quite rare

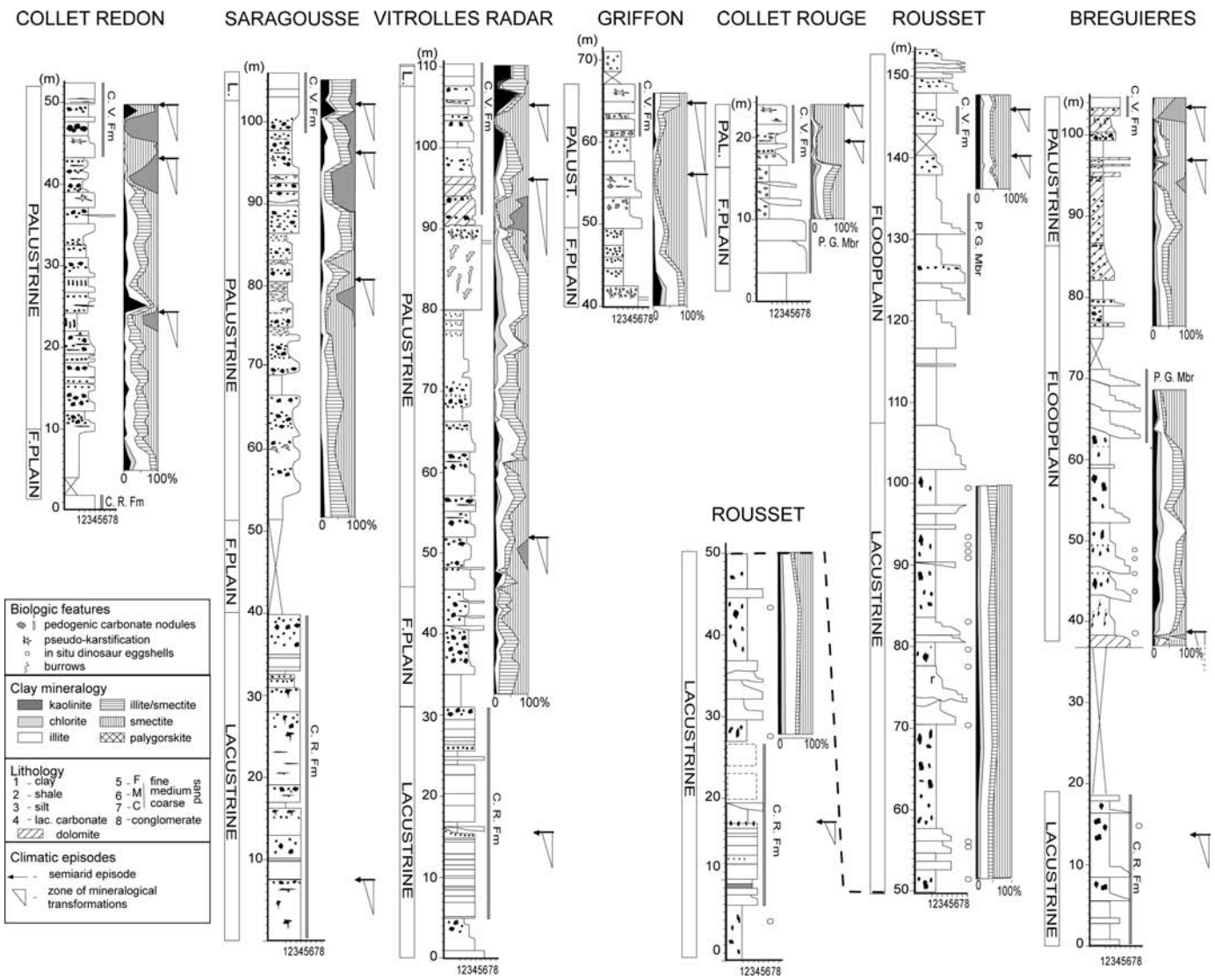

FIG. 4.—Lithology and clay-mineral assemblages from the studied sections (for section locations, see Fig. 1). Sections were measured (when possible) from the C. Rognac Formation up to the C. Vitrolles Fm. Clay mineralogy is indicated (this study; Colson 1996). Arrows refer to the semiarid episodes that were identified based on facies descriptions and clay-mineral assemblages.

(less than 10% of the studied interval thickness). The mineralogic study was conducted on several sections, including those sampled for the paleomagnetic study (Fig. 4).

Fine-Grained Facies.—*Micritic limestone beds* vary from 0.10 m to 0.60 m in thickness and are generally laterally extensive (up to a few kilometers). These facies do not show any stratification. The bases of the beds are sharp, and the upper surfaces show desiccation features, intraclasts, pseudo-karstification, root traces, and mottling. In the C. Rognac Fm, some beds contain numerous fossils of charophytes, gastropods, and ostracods. No fossils were found in the C. Vitrolles Fm. These micritic carbonates are composed of nearly 100% calcium carbonate with less than a few percent quartz and clay minerals. Clay mineralogy was not analyzed due to the very low concentration of clay minerals. This facies is interpreted as shallow lacustrine deposits. The evidence of subaerial exposure and the presence of root traces in these facies suggest a limited water depth that allowed growth of vegetation.

Carbonate deposits of limited lateral extent, a few hundred meters maximum. Two types of deposits have been identified: those isolated in the floodplain deposits, and those in relation with lacustrine micritic limestones. Deposits of the first type bear traces of subaerial exposure, including prismatic structures and pseudo-karstification. They may contain a significant amount of dolomite. Ghost shapes of gypsum and dolomite crystals that are replaced by calcite are apparent in thin sections. Clay-mineral assemblages consist of nearly pure smectites or mixed smectite–palygorskite (Colson et al. 1998). These deposits are interpreted as playa facies fed by groundwaters.

The other dolomitic facies are associated with a lake or a pond. They usually exhibit mottling, with rare nodules at the base. The number of nodules increases upwards, to form a coalescing horizon that passes at the top into massive dolocrete. Their clay content is generally low and never exceeds 20%. The composition of clay fraction progressively changes towards the most mature horizon, giving way to authigenic smectite and palygorskite (Colson and Cojan 1996). These deposits have been interpreted as resulting from the mixing of groundwater and lake brines

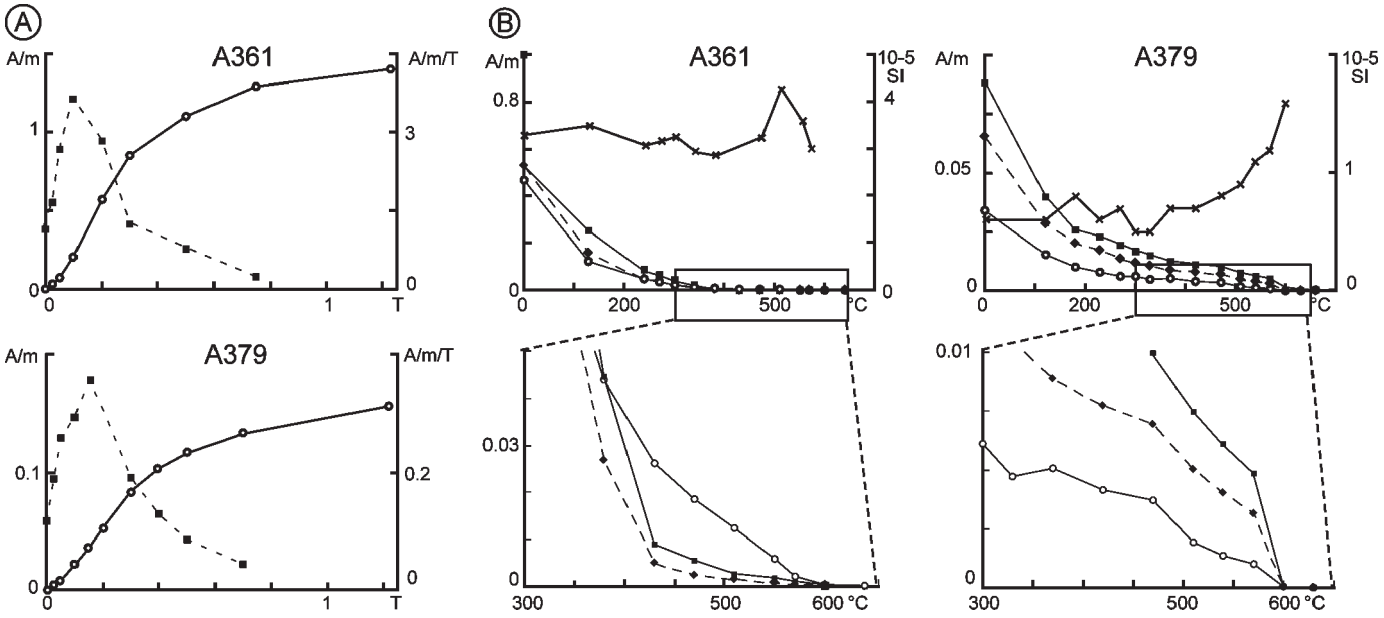

FIG. 5.—Rock-magnetic data from characteristic samples (sample A361, VI section, 59 m; sample A379, CR section, 5 m). **A)** IRM acquisition from 0 to 1.2 T. Open circles, IRM; solid squares, derivate of IRM. **B)** Stepwise thermal demagnetization of three-component IRM (Lowrie 1990). Lower diagram corresponds to a zoom on the end of the demagnetization. Open circles, soft component (0.12 T); solid squares, medium component (0.4 T); solid diamonds and dashed line, hard component (1.2 T); crosses, evolution of low field volumetric magnetic susceptibility.

during periods of strong evaporation and lake-level lowering. They are named groundwater dolocretes (Colson and Cojan 1996). The dolocrete development is topographically controlled. On low-lying lake margins, a palustrine limestone and dolocrete assemblage developed, while a calcrete and dolocrete assemblage formed on topographically high lake margins.

Lignite beds, typically about 0.10 m thick, do not have well defined contacts. They are interbedded with gray to green clay layers which are often disrupted by root traces. This facies is always developed on top of lacustrine carbonates. These deposits are restricted to the C. Rognac Fm (RO and VI sections). The lignite beds reflect periods of low fluctuations of the lake level or the water table, favorable to the preservation of organic matter.

Shales and siltstones make up more than 80% of the succession. Contacts between the deposits are fuzzy, and grading is absent. These fine-grained facies often bear traces of mottling. Colors range from drab to reddish. Black nodules of iron and manganese can be found in association with pink to purple colors (BR section). Bioturbation is quite abundant in some horizons. Numerous carbonate nodules associated with slickensides are present in most of these horizons. Shales and siltstones are composed of 40 to 60% calcium carbonate, up to 40% clay, and no more than 20% quartz. The high proportion of carbonate is a distinctive aspect of these successions (Cojan 1999). The average clay-mineral association of the floodplain silts deposited close to the channel belt is dominated by illite, interstratified illite–smectite, and smectite (Cojan 1999) (Fig. 5). Clay minerals also include minor amounts of chlorite, kaolinite, and palygorskite as well as mixed-layer varieties such as chlorite–smectite.

These fine-grained sediments accumulated on the floodplain during widespread overbank flooding associated with high-discharge periods. After deposition, stratification was disrupted by pedogenesis. Two types of paleosols have been identified: carbonate-rich and pseudo-gleyed. The absence of large sand bodies in the studied interval is interpreted as a consequence of expansion of the lake area because of migration of the channel belt to the south of the study area, where time-correlative strata are now eroded. As a result of pedogenesis: (1) the proportion of carbonate increased with distance from the channel belt while the proportion of quartz decreased due to selective preservation of b_c horizons (carbonate accumulation horizon), and (2) the proportion of illite decreased due to replacement by interstratified illite–smectite, smectite, and palygorskite (Colson et al. 1998).

Coarse-Grained Facies.—*Sandstones* are quite rare in the studied interval. They are restricted to the eastern part of the basin and are interbedded either with the lignitic or clayey facies, or reddish shales or siltstones. They occur as isolated channel fillings that are typically < 5 m wide and < 5 m thick. They display a sharp erosional base, upward fining, and trough cross-stratification. Other sand bodies correspond to multi-layer sheet bodies that extend hundreds of meters laterally. These deposits have sharp bases with no evidence of erosion and progressively fine upward into silty sediments. These are interpreted as river-generated mouth bars or splays.

Conglomeratic units are composed of several stories of sheet deposits with limited erosional features. Occurrence of this facies is also limited to the eastern part of the basin, where they are intercalated within red shales or siltstones. The grain size ranges from coarse-grained sand to well rounded clasts less than 0.10 m in size that are derived from distant sources. Clast imbrication and crude cross-stratification are frequent. Bulk-rock mineralogy of conglomeratic deposits was determined on the fine-grained fraction. Clay minerals include illite with some interstratified smectite–illite, attesting to the freshness of the material from which these deposits originated. The conglomeratic assemblages were deposited in a river-dominated distal alluvial fan. Fan sediments were derived from the Maures Massif, located some 60 km away from the study area.

Lake and floodplain environments are represented in all sections but alluvial fans are restricted to the BR section.

Paleomagnetism

For the paleomagnetic study, the following facies were sampled: white to drab lacustrine limestones, pink to reddish palustrine carbonates, and

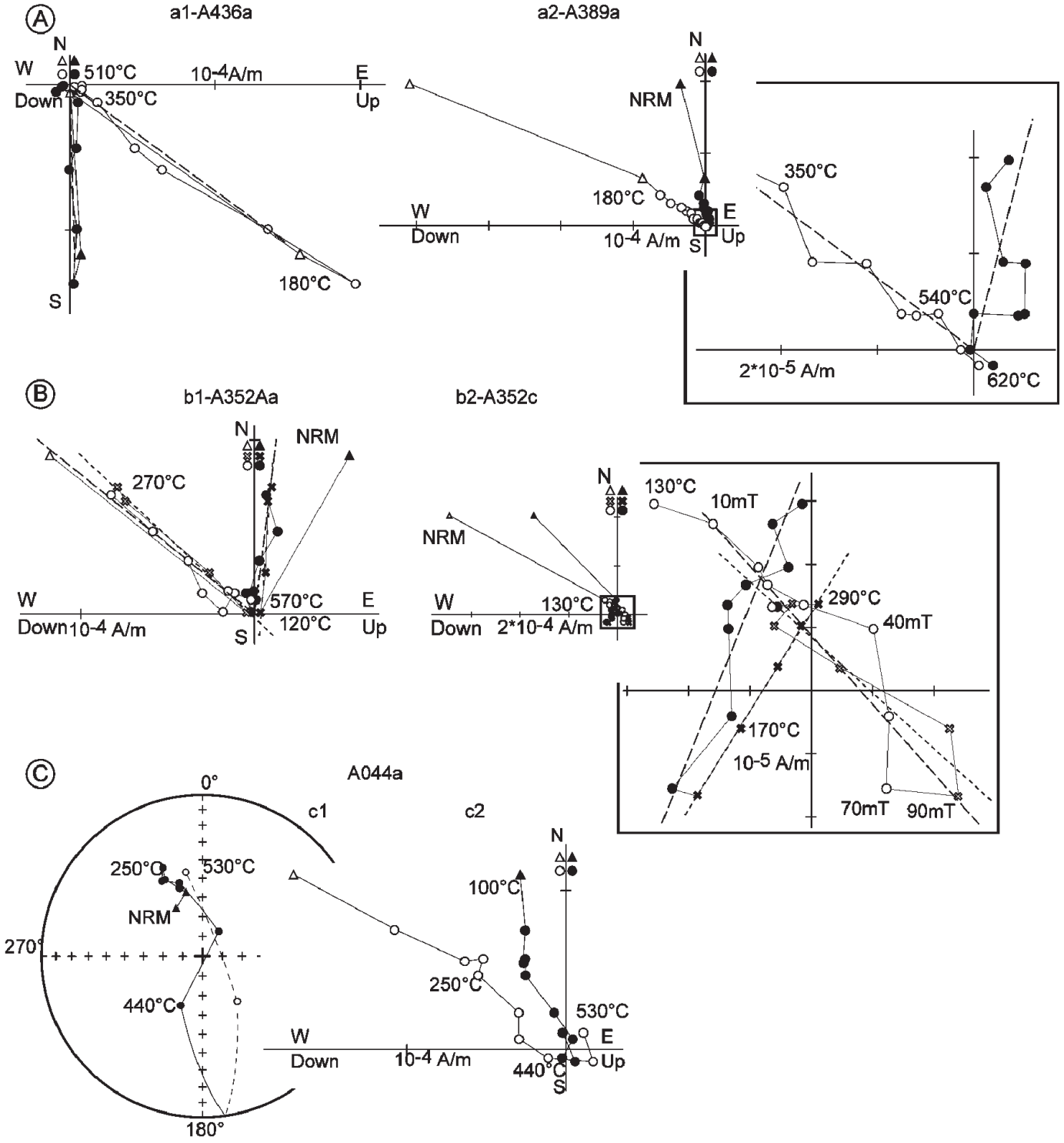

FIG. 6.—Representative diagrams of demagnetization path. In the orthogonal vector projections: solid/open symbols, horizontal/vertical plane; triangles, first component parallel to present field; crosses and fine dotted line, low unblocking-temperature (lt) component removed between 270 and 350°C; circles and large dotted line, high-temperature (ht) component stable up to 510–610°C (thermal) or to 50–90 mT (alternative field). Framed diagrams correspond to a zoom on the end of the demagnetization. **A)** Samples with only one stable component: a1—Reversed polarity (sample A436a, CR section, 35.8 m), a2—Normal polarity (sample A389a, CR section, 11.7 m). **B)** Sister samples with two antipodal stable components (sample A352, VI section, 46 m): b1—Thermal demagnetization path showing reversed component between 120°C and 270°C (crosses and fine dotted line) and a normal component between 300 and 570°C (circles and heavy dotted line). b2—Combined alternating field (crosses) and thermal (circles) demagnetization path showing a normal component between 10 and 90 mT (heavy dotted line) and a reversed component between 170°C and 290°C (fine dotted line). The remaining unstable normal polarity component is not shown. **C)** Sample that does not permit isolation of a stable component (sample A044A, GR section, 57 m). c1—Equal-area projection (solid/open symbols; lower/upper hemispheres, respectively). Demagnetization path seems to fit a great circle. c2—Orthogonal projection of thermal demagnetization.

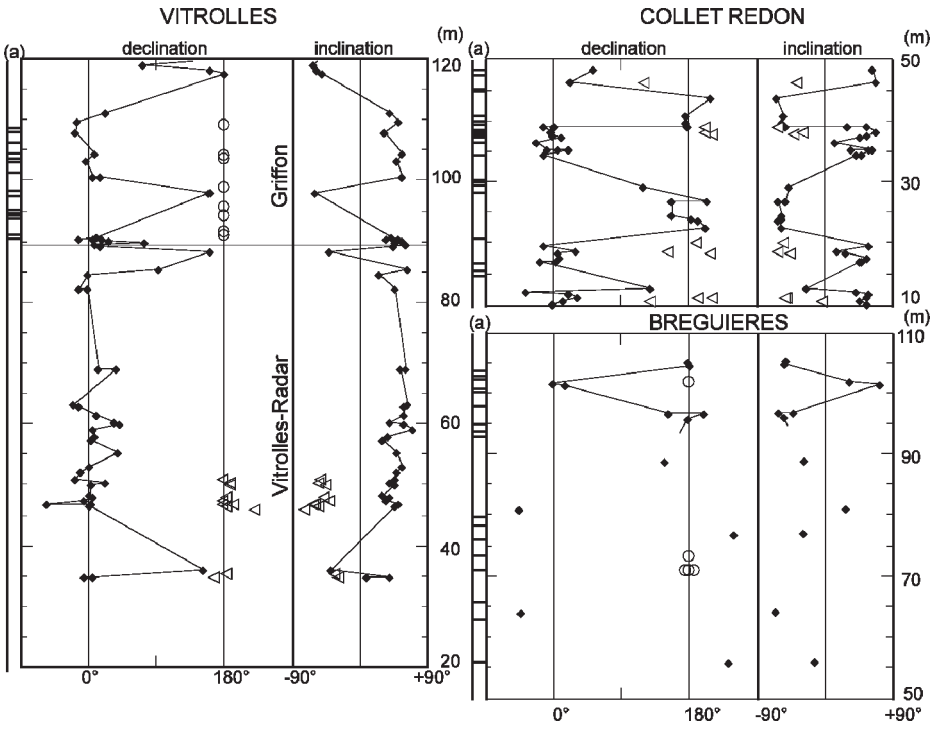

FIG. 7.—Stratigraphic plot of paleomagnetic results from Vitrolles Radar (VI), Griffon (GR), Collet Redon (CR), and Bréguières (BR) sections. For section locations see Figure 1. Results from VI and GR section are presented on the composite Vitrolles section (0 m on GR section corresponds to 89.75 m on composite section). Column a, samples without a stable remanent component; diamonds, ht component; triangles, lt component; open circles, samples with demagnetization circles.

muddy to silty paleosols. Sandy and coarse-grained facies were avoided. Intensities of natural remanent magnetization (NRM) vary between 0.01 and 10 mA/m. The least magnetized samples are purely white lacustrine limestones; samples with the highest intensities are reddish paleosols. For 90% of the samples, intensity of natural remanent magnetization was high enough to obtain interpretable data.

Magnetic Carriers.—IRM experiments were carried out by submitting samples to a continuous field of up to 1.2 Tesla at ambient temperature. Saturation was never reached, indicating the presence of high coercivity carriers such as hematite or goethite (Fig. 5A). Due to the presence of high-coercivity carriers, alternating-field (af) demagnetization was largely unsuccessful. Thermal demagnetization shows a partial destruction of a hard component at 120°C (Fig. 5B), which is attributed to goethite. Above this temperature, thermal demagnetization curves of all three components are very similar, and never showing a steep slope, with a maximum unblocking temperature between 500 and 650°C (Fig. 5B). The rapid demagnetization of hard and medium components near 600°C may be the result of a mineralogic transformation, perhaps due to the reduction of hematite into magnetite, as suggested by the increase of susceptibility (Fig. 5B, sample A379). Following these analyses, the main magnetic carrier was interpreted to be fine- to coarse-grained hematite particles. Nevertheless, the presence of magnetite is suggested in some samples by a steep decrease of the soft component near 580°C (Fig. 5B).

Natural Remanent Magnetization.—Thermal demagnetization was routinely applied. All samples possess a magnetization component that is parallel or anti-parallel to the present field, which is removed at 120–180°C (Fig. 6). After this heating, the magnetization intensity can be less than 0.02 mA/m. Most samples show only one normal or reverse component that is slowly unblocked between 120 and 500–620°C (Fig. 6A). Some samples show a complex magnetic signal that often possesses three components (Fig. 6B). On representative samples (Fig. 6B, sample A352A), a first component, approximately parallel to present field, is completely removed at 120°C and is probably carried by goethite. An additional, well-defined (linear), lower unblocking temperature component is removed around 270–350°C. Above 270–350°C, the magnetization intensity is often less than 0.02 mA/m. The third component, stable up to 570–610°C, is anti-parallel to the second one and is interpreted as normal polarity. The component that is characterized between 120 and 350°C will be called the "lower temperature (lt) component" and that above 350°C the "high temperature (ht) component" throughout the remainder of this paper.

Mineralogic studies did not reveal the presence of pyrrhotite which could have explained the low-temperature reverse component. Magnetic carriers in samples with three components (e.g., Fig. 6B) were investigated using combined thermal and alternating-field demagnetization; these experiments were carried out on sister samples. After heating samples to 130°C to destroy the magnetization carried by goethite, the samples were then stepwise af demagnetized with maximum fields up to 90 mT, which isolated a component that is always of normal polarity. It is approximately parallel to the ht component of the sister sample. This component, stable up to 570–600°C and removed by af demagnetization, is at least partially carried by magnetite. After af demagnetization to 90 mT, the same sample was heated stepwise between 170 and 300°C, which isolated a reverse polarity component interpreted to be carried by very small grains of hematite on the basis of the low unblocking temperature and high coercivity. The magnetization directions above 300°C become very unstable. These results are consistent with the presence of mixed magnetite and hematite carriers for the normal high blocking temperature component and only very small hematite grains for the low blocking temperature reversed component.

For thirteen specimens, most of which come from the Vitrolles section, no direction could be calculated by means of least-squares regression because demagnetization paths from these samples seemed to follow a great circle path, which suggests a change from normal to reverse polarity during demagnetization. (Fig. 6C).

Paleomagnetic Results.—The paleomagnetic results obtained on the four sampled sections are presented for each section in Figure 7.

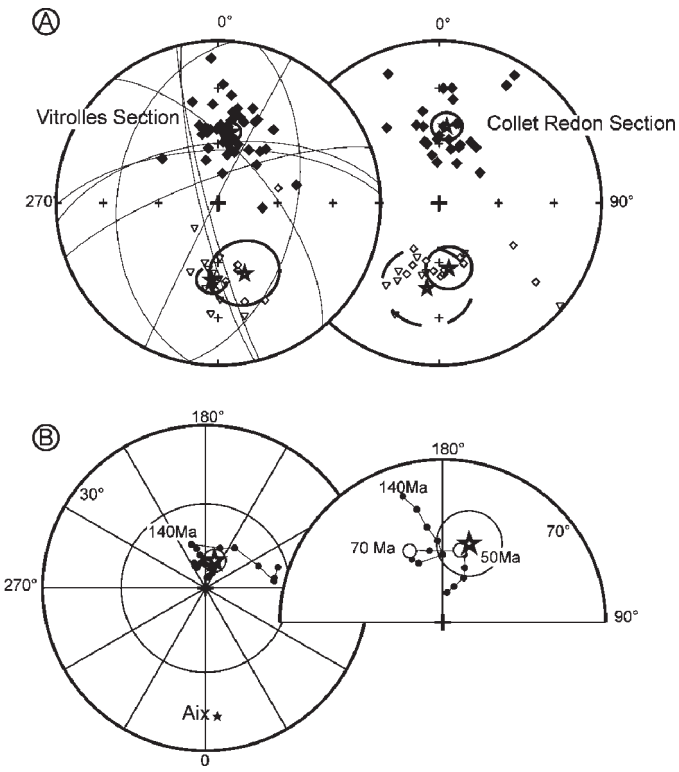

FIG. 8.—**A)** Equal-area projection of characteristic components, demagnetization circles, and means from Vitrolles and Collet Redon sections. Solid/open symbols, down/up directions; only the upper half of demagnetization circles are shown. Diamonds, ht component; triangles, lt component; stars, means; confidence circles (solid line, ht component; dashed line, lt component). **B)** Comparison of VGP (virtual geomagnetic pole) from the Upper Cretaceous formations from the Aix-en-Provence basin (star with confidence cone) with European APWP (Besse and Courtillot 2002). The zoom shows that latitude of the VGP from the location is in accordance with European APWP around 50 to 70 Ma.

The Collet Redon section is located in the western part of the basin (Fig. 1). It is dominated by palustrine facies. Most samples show only one normal or reverse component that is slowly removed between 120 and 500–620°C. Nevertheless, some samples show two components, a reversed polarity that is removed at up to 400°C and a normal polarity that is removed around 500–620°C. Seven polarity intervals are defined by high-temperature components.

The Vitrolles section is a composite section that corresponds to the base of the Vitrolles-Radar section (up to 89.25 m) and the upper part to the Griffon section. Both sections are well correlated on the basis of facies and mineralogy.

The Vitrolles-Radar section is located some 10 km south of the Collet Redon section (Fig. 1). In the lower part of the section, numerous silty paleosols are interbedded with palustrine facies. Up to 51 m, the magnetic signal is complex and often possesses three components. Nevertheless, the sample at 36.2 m shows a reverse component that is stable up to 510°C and no high temperature normal polarity is observed. Above, up to the top of the VR section (89.25 m), stable magnetization directions are defined between 250 and 600°C. Above this temperature, remagnetization brings noise into the signal. Magnetic directions are of normal polarity except for a sample at 88.5 m.

The Griffon section is situated some 5 km southeast of Vitrolles-Radar section. A stable normal polarity component is defined up to 500–600°C for seven specimens between 89.75 and 90.75 meters. Above, up to 100 meters, demagnetization diagrams are very noisy. Nevertheless, demagnetization paths for seven samples seem to fit a great circle, which suggests a change from normal to reverse polarity during demagnetization (McFadden and McElhinny 1988) (Fig. 6C). The sample at height 97.75 m displays a well defined reversed polarity. We suggest that these samples were magnetized during a reversed-polarity interval and subsequently contaminated by a normal polarity. The interpretation of a reversed polarity for primary magnetization is then proposed between 90.75 and 100 meters stratigraphic height. Above, up to 111.15 m, a third of the samples are too noisy to be interpreted. Seven samples show normal polarity, but three samples exhibit remagnetization circles. This 11.15 m interval is probably of normal polarity, but we cannot exclude the possibility of a recent remagnetization.

Along the composite Vitrolles section up to 100 meters, six polarity intervals are proposed on the basis of the high temperature components (Fig. 7).

The Bréguières section is located in the eastern part of the basin (Fig. 1). It is dominated by red shaly to silty deposits. Twenty-one out of the 38 samples show very intricate diagrams without a defined component above 150°C. Between 250 and 550–600°C, 12 samples out of the 17 remaining samples show crudely defined components (Fig. 7), nine with reversed polarity and three (101.5, 101.75, and 81 m) with normal polarity. Demagnetization paths of five samples fit a great circle (Fig. 7). Hence, no magnetic sequence is proposed for this section.

TABLE 1.—*Mean directions for the lt and ht stable components (CR and VI sections).*

Site	n	Dg (°)	Ig (°)	Ds (°)	Is (°)	k	α_{95} (°)
CR section							
lt component	8	188.0	−45.1	188.1	−46.0	7.7	21.3
ht component N	27	5.5	49.7	5.7	50.6	15.8	7.20
ht component R	12	171.7	−55.6	171.5	−56.6	16.4	11.0
VI section							
lt component	13	184.7	−49.7	184.8	−50.7	34.0	7.20
ht component N	43	9.9	52.9	9.9	53.3	20.8	4.90
ht component R	7	159.6	−51.5	159.5	−51.6	13.6	17.0
Means component							
normal	70	8.100	51.7	8.2	52.3	18.7	4.0
reversed	40	178.0	−51.7	178.0	−52.5	14.3	6.2
mean	110	4.500	51.8	4.6	52.5	16.6	3.4
Poles							A95
	110	161.9	79.6	160.1	80.2	12.6	3.9

n = number of samples; Dg/Ig declination/inclination in geographic coordinates; Ds/Is declination/inclination in tilting corrected coordinates; k, α_{95} Fischer statistical parameters.

Calculation of Site-Mean Directions and Age of Magnetization

For the Collet Redon and Vitrolles sites we plotted all stable components or demagnetization circles (Fig. 8A). Mean directions were calculated for lt and ht components (Table 1). Data from demagnetization circles were removed before calculation. For all samples, lt and ht mean directions are the same or antipodal, suggesting that ht and lt magnetizations were acquired over a short time (McFadden and McElhinny 1990).

For the two sites dip is around 1° to the south and a fold test is not significant. Latitude of the VGP (virtual geomagnetic pole) calculated from the average of all components is in accordance with the European APWP from about 50 to 70 Ma (Besse and Courtillot 2002) (Fig. 8B). Moreover, for the Vitrolles section, identification of mixed magnetite and hematite carriers for the normal ht component suggests detrital or early post-depositional magnetization. We interpret the ht magnetizations as primary.

The magnetic direction expected at 65 Ma for the location based on the APWP of Europe is DEurope = −2.4° ± 5.4° and IEurope = 53.7° ± 3.2°, and the direction defined by this study is D = 4.6° ± 6.3° and

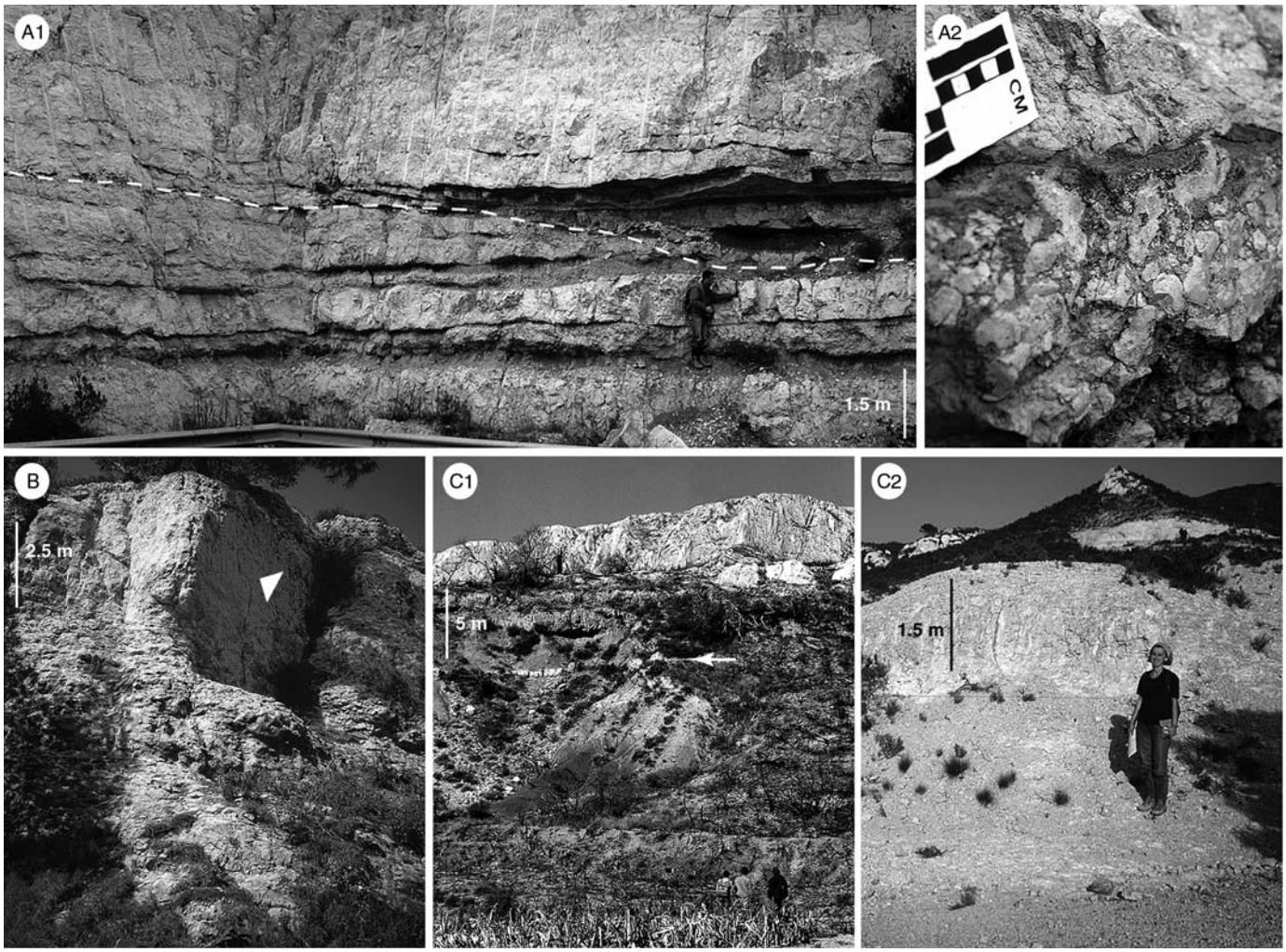

FIG. 9.—Illustration of the various facies associated to the semiarid episodes. **A)** Lacustrine deposits. A1—Incision related to tributaries that flowed into the lake. During low lake levels, incisions that are several tens of meters wide and a few meters deep were scoured into the micritic lacustrine carbonates (VI section, episode 1, incision surface is indicated by the dashed line). A2—In situ brecciation. Intraclasts that formed during subaerial exposure of the lacustrine carbonates were not displaced. Deep brecciation, to more than 20 cm, and ferruginous accumulations in the spaces between the clasts are associated with subaerial exposure (VI and RO sections, episode 1). **B)** Marginal lacustrine environment. The groundwater dolocrete commonly does not display sharp contacts. The central part of the dolocrete corresponds to the massive carbonate level (white arrow). The nodular textures correspond to the upper and lower contacts of the dolocrete (VI section, episode 4). **C)** The floodplain. C1—A playa deposit that corresponds to a lens of micritic carbonate (arrow). Bed thickness does not exceed a meter, and the bed extends over a few hundreds of meters. Scattered gypsum and dolomite crystal moulds are abundant (BR section, episode 4). C2—A mature carbonate-rich paleosol. The nodules of the rhizomorphs are close to coalescence, mimicking a palustrine facies. Reddish mottling is indicative of strong pedogenesis (CR section, episode 2).

$I = 52.5^\circ \pm 4^\circ$, suggesting a $7.0^\circ \pm 13^\circ$ rotation. This rotation is likely the result of sinistral strike-slip movement of the Aix-Fault system since deposition (Gaviglio 1987).

DISCUSSION

The Aix-en-Provence continental sedimentation is considered to have taken place in an endoreic low-lying basin fed by an axial fluvial system locally bounded by transverse fans. Spatial and temporal changes in the depositional environments reflect climate change, although differential subsidence is recorded by thickness variation of the correlated intervals. Time-significant correlations are based on paleomagnetic data.

Evidence of Climatic Fluctuations

The overall depositional pattern suggests a warm climatic setting. Rainy periods alternated with seasonally dry periods during which carbonate-rich paleosols developed in floodplain alluvium and shallow lacustrine deposits were subaerially exposed.

Within this general context, some periods characterized by more evaporative semiarid conditions have been identified on the basis of field observations, macrofacies and microfacies descriptions, and mineralogic studies. Semiarid conditions are reflected across a toposequence, from the main lake body towards the floodplain (Figs. 9, 10).

(1) Towards the central part of the permanent lake, micritic lacustrine beds accumulated during subhumid periods. During the semiarid episodes, the lowering of the lake level associated with changes in the hydrologic balance is represented by scours of up to 2 m where tributary channels flowed into the lake (Fig. 9A1). The low lake levels are also recorded by deeply brecciated bed surfaces with some pseudo-karstification (Fig. 9A2). No mineralogic transformations have been identified.

(2) Along the margins of the lake body, the micritic lacustrine beds were subjected to limited subaerial exposure during the subhumid

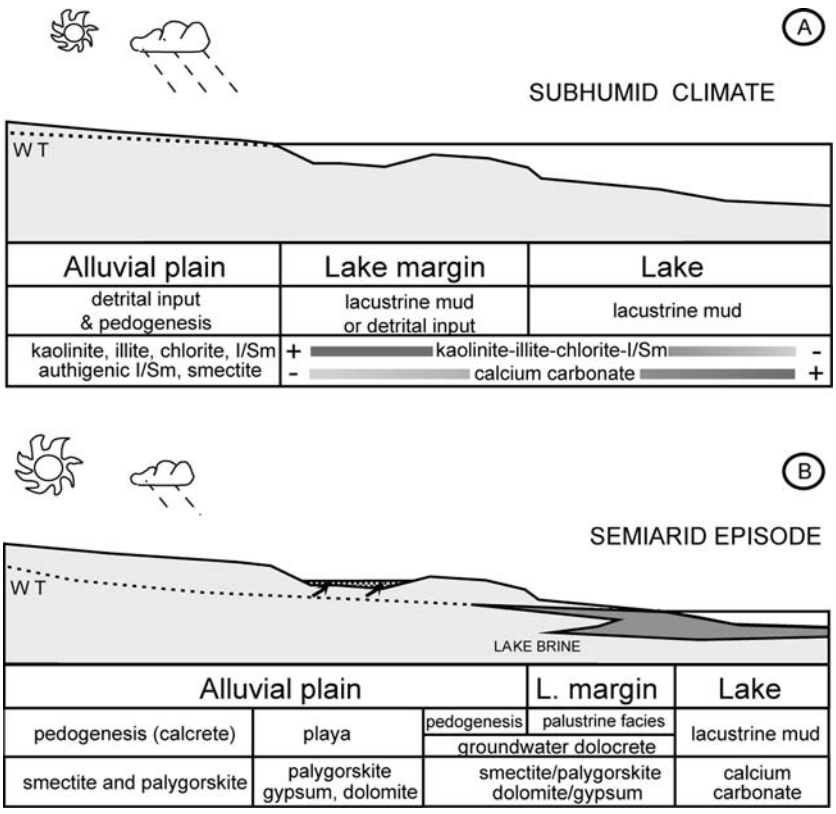

FIG. 10.—Schematic diagram illustrating the distribution of facies along the catena in response to climatic changes (WT, water table). **A)** Subhumid climate, with alternating wet and dry seasons. Overbank alluvium and channels fill in the floodplain and carbonate mud is deposited in the shallow lake. Pedogenesis resulted in carbonate-rich paleosols with limited mineralogical transformations. **B)** Semiarid episode: pedogenesis and precipitations from groundwater are dominant over most of the area.

periods. When the main lake body was restricted to its minimal size, during the semiarid episodes, a groundwater dolocrete formed close to the permanent lake deposits, either on the floodplain deposits or on the lake-margin sediments (Colson and Cojan 1996).

(3) In the floodplain, carbonate-rich paleosols of limited development are present during the subhumid conditions. Development of mature carbonate-rich paleosols with a large proportion of authigenic clay minerals was promoted during the semiarid episodes (Fig. 9C2). These mature calcretes contain more or less coalescent nodules displaying typical circumgranular cracks. Partly authigenic smectites are dominant clay minerals, but occurrence of palygorskite is a good indicator of evaporative conditions. The low-lying areas of the floodplain were occupied by playa lakes of limited extent (Fig. 9C1). The associated deposits are most often composed of micritic dolomite showing ghosts of gypsum crystals. Associated clay minerals are smectite with a significant amount of palygorskite.

On the basis of facies, pedogenic, early diagenetic, and mineralogic characteristics, it is proposed that under subhumid conditions, sediment accumulation was the major process and mineralogic transformations were limited (Fig. 10). During semiarid episodes, pedogenesis and evaporative deposition dominated, resulting in facies rich in dolomite, smectite, and palygorskite. Facies with clay mineralogy dominated by smectite may not be indicators of semiarid conditions only; they may also reflect long periods of pedogenesis under stable climatic conditions.

Following the above-mentioned criteria, four semiarid episodes were identified from the record of the Bréguières, Collet Redon, Vitrolles-Radar, and Saragousse sections (Fig. 5). Three semiarid episodes were identified in the Rousset section, and only two semiarid episodes were present in the Griffon and Collet Rouge sections. The semiarid deposits constitute key horizons that are used to correlate the sections.

Acquisition of the lt Paleomagnetic Component

Record of the semiarid episodes is investigated from the paleomagnetic signal. In the following, the complex paleomagnetic signal is interpreted on the basis of the facies and mineralogic description.

Paleomagnetic directions (both lt and ht components) of the samples were converted into virtual geomagnetic poles (VGP). VGP latitudes are plotted in Figure 11 as a function of stratigraphic position. Data from the Collet Redon section are shown in stratigraphic order:

(1) A first set of samples with a lt reverse component (10–12 m) is overlain by a reverse ht sample (12.5 m). This paleomagnetic record is associated with a quite mature reddish paleosol (paleosol top at 12 m) that is rich in illite–smectite and smectite.

(2) The second (18.5–20 m) and third (28–28.5 m) set of samples with a reverse lt component are from zones of mineralogic transformation corresponding to semiarid episodes. Both of these semiarid episodes happened during reverse ht intervals, and mineralogic transformations associated with these episodes extend down into the upper part of a ht normal interval.

(3) The fourth set (46.5 m) contains only one sample with a lt component. It coincides with a semiarid episode that occurred during a normal ht polarity sequence.

It is interesting to note: (1) the limited stratigraphic extent of samples with a lt component (less than 2 m in CR section, up to 5 m in VI section), (2) the strong correlation between samples with a lt component and the occurrence of mineralogic transformations associated with semiarid episodes within ht reverse polarity intervals.

Cathodoluminescence examination of the samples possessing lt components (dominantly palustrine carbonates) indicates that the original sediment exhibits a dull luminescence but calcite recrystallizations show a succession of bright and dull color stripes (Fig. 12B, C). It is

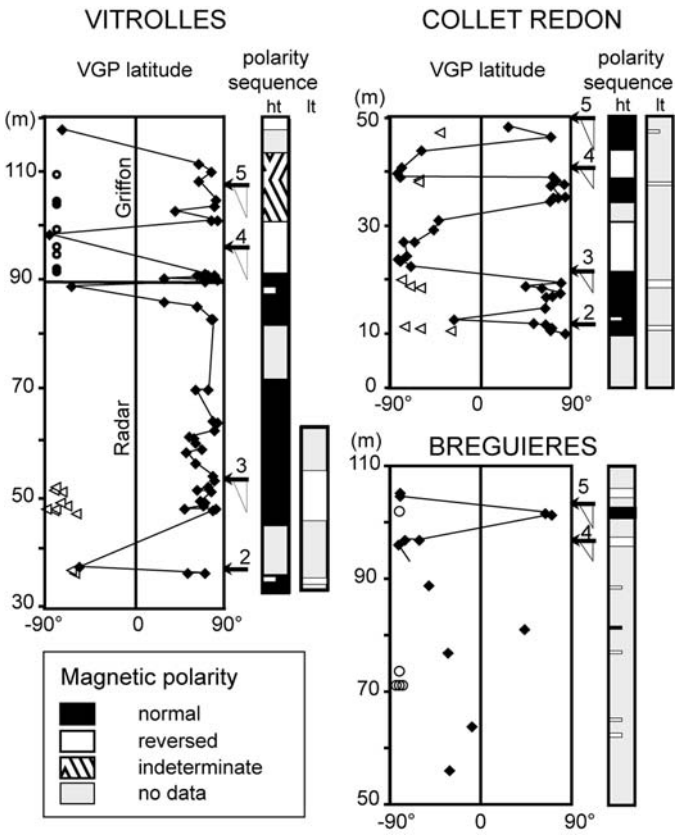

FIG. 11.—Polarity sequences and climatic data for Vitrolles (VI), Collet Redon (CR), Bréguières (BR), and sections (see Fig. 1 for section location). For each section, semiarid episodes (arrow), zone of mineralogical transformation (elongated triangle), VGP latitude (diamond, ht component; triangles, lt component) and magnetic polarity of the ht and lt sequences are displayed. On VI and BR sections, open circles indicate samples with demagnetization circles.

proposed that these crystals developed from fluids (groundwater or percolating water) with variable Eh. Thus, we suggest that the lt component was acquired after sediment deposition, as a result of fluid circulation. Percolating fluids with varied oxidizing potentials would have enabled the growth of magnetic minerals such as fine-grained hematite. This interpretation is in agreement with the rock-magnetic study. Very small hematite grains are the lt magnetic carrier in the studied interval.

The complex paleomagnetic signal observed in the stratigraphic sections can then be explained by climatic fluctuations (Fig. 13). During sedimentation, magnetization is detritico-diagenetic. The magnetic signal is carried by hematite or magnetite with an unblocking temperature up to 620°C. Under subhumid climatic conditions, emergent periods are limited in time, sedimentation is nearly continuous, and the original signal is preserved (Fig. 13A1). On the contrary, during semiarid episodes, the duration of exposure is longer. Lowering of the water table allowed percolation of water to depths of several meters, creating favorable conditions for diagenetic processes such as calcite dissolution or reprecipitation, or alternating reducing-oxidizing conditions (Fig 13A2). These diagenetic processes promote development of very fine-grained hematite (unblocking temperature up to 400°C). The overprint is antipodal to the primary magnetization if a magnetic field reversal occurred between the times of sedimentation and diagenesis (Fig. 13B).

On the basis of the stratigraphic distribution of the mineralogic transformations associated with the semiarid episodes and the lt magnetic components, we propose that five semiarid episodes are present along the study interval (Fig. 14): the first one is identified in the C. Rognac Fm on the basis of erosional and pedogenic feature (no paleomagnetic data available) (SA, VI, RO, BR), the second one is based on paleomagnetic data (CR, VI, BR), and the third, fourth, and fifth are defined from mineralogic transformations and lt paleomagnetic component (SA, VI, RO, CO, BR).

Data from the Vitrolles section are similar, but the record of the semiarid episode 3 in the Vitrolles section is puzzling: the samples with a lt component are not overlain by a reverse ht interval. Because the sample density is high over this interval, we propose the occurrence of a sedimentation break above or within the third episode in the Vitrolles-Radar section (a hiatus or some erosional features).

Magnetostratigraphy

A magnetostratigraphy based on our observations and previously published data has been constructed in order to complement sparse biostratigraphic data.

Western Part of the Basin.—Paleomagnetic results are available for three sections (Fig. 1): the Collet Redon section (CR; Cojan et al. 2000, this study), the Saragousse section (SA; Galbrun 1989; Galbrun et al. 1991), the Vitrolles-Radar section (VI; Westphal and Durand 1990, this study) and the Griffon section (GR; this study) (Fig. 14). Data from the Saragousse section are not discussed here because all the reverse components were determined at temperatures below 240°C, the unblocking temperature of the lt component, and because the normal ht components are close to the present field (Galbrun 1989).

In terms of magnetostratigraphy, the ht polarity sequences of the CR section offer the most complete ht signal with seven polarity reversals. On the basis of a previously defined magnetostratigraphy and chemostratigraphy, the upper ht reverse interval of the Collet Redon section is correlated with chron 29R (Cojan et al. 2000). Semiarid episode 3 is located within this chron.

Although the exact position of the magnetic-field reversals are not typically well defined, the following magnetostratigraphy is proposed from bottom to top based on the combination of the paleomagnetic data with the sedimentologic record of the semiarid episodes in the three available sections:

(1) the N–R–N sequence from the C. Rognac Fm (semiarid episode 1) is correlated with the base of anomaly 32 (VI section, Westphal and Durand 1990),
(2) the overlying predominantly normal polarity interval (semiarid episode 2) corresponds to the upper part of anomaly 32 (CR section 10 to 21 m, VI section 33 to 53 m),
(3) a reverse interval (semiarid episode 3) is ascribed to chron 31R (CR section 21 to 31 m, VI section overprint down from 53 m),
(4) a stratigraphically higher predominantly normal-polarity interval is interpreted as representative of the succession 31N–30R–30N (CR section 35 to 40 m, VI section 53 to 90 m),
(5) the overlying reverse interval (semiarid episode 4) is correlated with chron 29R (CR section 40 to 45 m, VI section 92 to above 100 m),
(6) the normal interval (semiarid episode 5) is correlated with C29N–28R–28N (CR section 45 to 50 m, VI section between 100 and 115 m),
(7) the uppermost reverse chron corresponds to 27R (GR section above 115 m) (Cojan et al. 2000).

These correlations indicate large contrasts in thickness within the lower parts of the Vitrolles, Collet Redon, and Saragousse sections, while the sedimentary record is of fairly equal thickness in the upper part of the sections. This suggests the basin underwent synsedimentary deformation.

Eastern Part of the Basin.—In the eastern part of the basin, paleomagnetic results are available from three sections (Fig. 1): Collet

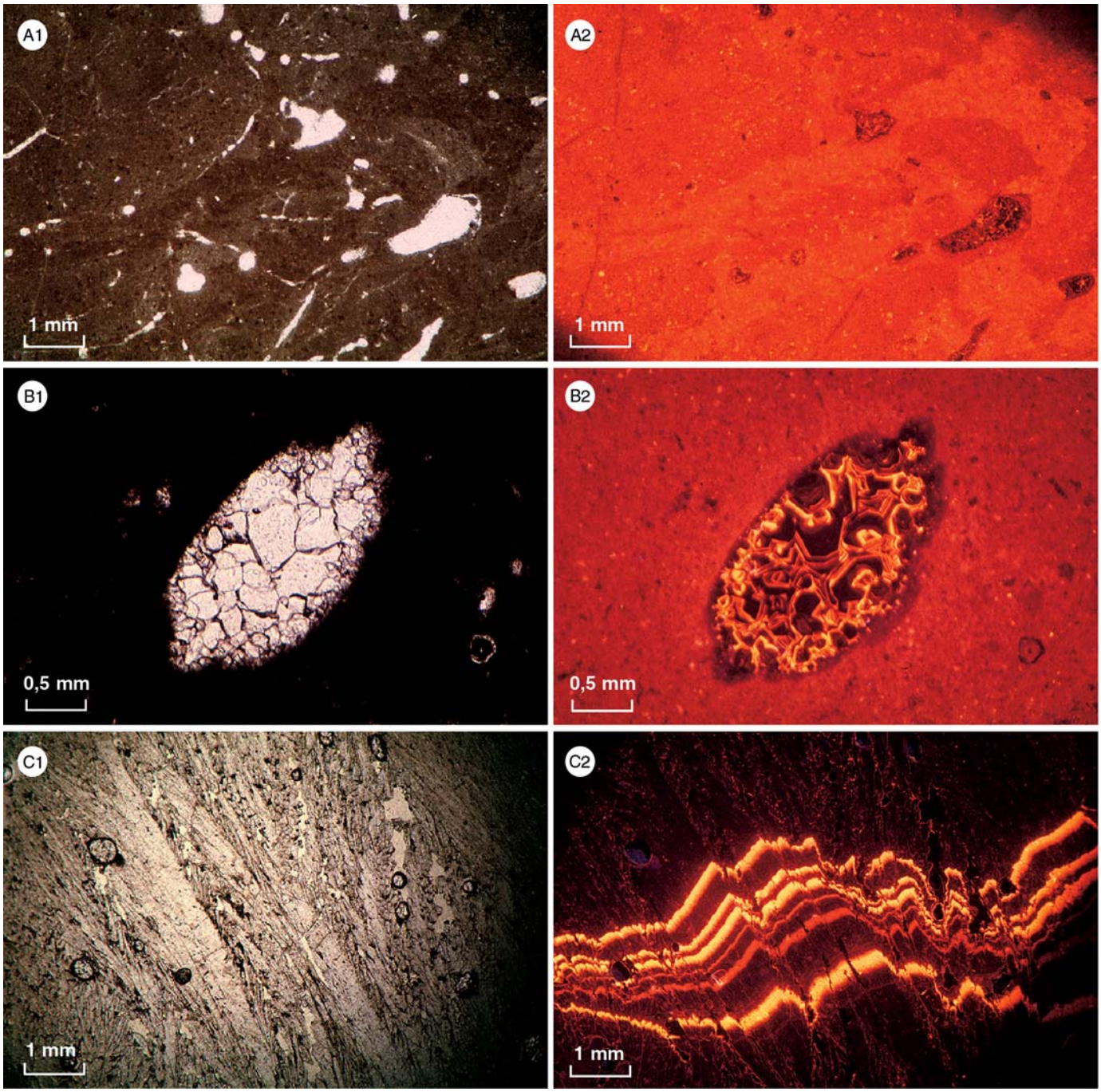

FIG. 12.—Cathodoluminescence investigation of calcite recrystallization in palustrine facies. The concentric pattern of zoning in calcite cements reflects changes in the composition of circulating fluids (meteoric vadose or phreatic). (1, transmitted light photomicrograph; 2, cathodoluminescence photomicrograph). **A)** Subhumid climate: micritic carbonates present a dull to moderate luminescence. Pedoturbation is distinct in color from the background sediment (CR section, 15 m). **B)** Semiarid episode (episode 3): Detail of a cement that recrystallized in a void as a consequence of decay of plants or pseudo-karstification. The cement crystals show nonluminescent zones separated by moderate to bright luminescent zones (CR section 19.5 m). **C)** Semiarid episode (episode 3): concentric pattern of zoning in calcite crystals (VI, 49 m).

Rouge (CR) (Westphal and Durand 1990), then Rousset (RO) (Krumsiek and Hahn 1989, Westphal and Durand 1990) and Bréguières (BR) (Galbrun 1997; this study). These sections are tied together by several horizons that are physically correlated: (1) the emergence surface corresponding to semiarid episode 1, (2) the Poudingue de la Galante Member (P. Galante Mbr), (3) semiarid episodes 4 and 5, represented by playa facies, paleosols, or groundwater dolocretes, depending on the location of the section in the toposequence.

The Rousset section possesses the only paleomagnetic data covering the C. Rognac Fm (Fig. 14). It shows a sequence of N–R–N–R–N that is correlated with anomaly 32 (Westphal and Durand 1990). Above, the Argiles Rutilantes Fm up to the P. Galante Mbr is a R–N sequence (Krumsiek and Hahn 1989; C. Kissel unpublished data). It can be attributed to anomaly 31 or the 31R–30N sequence.

The Collet Rouge section (Fig. 14) is well tied to the Rousset section through correlation of the P. Galante Mbr and semiarid episodes

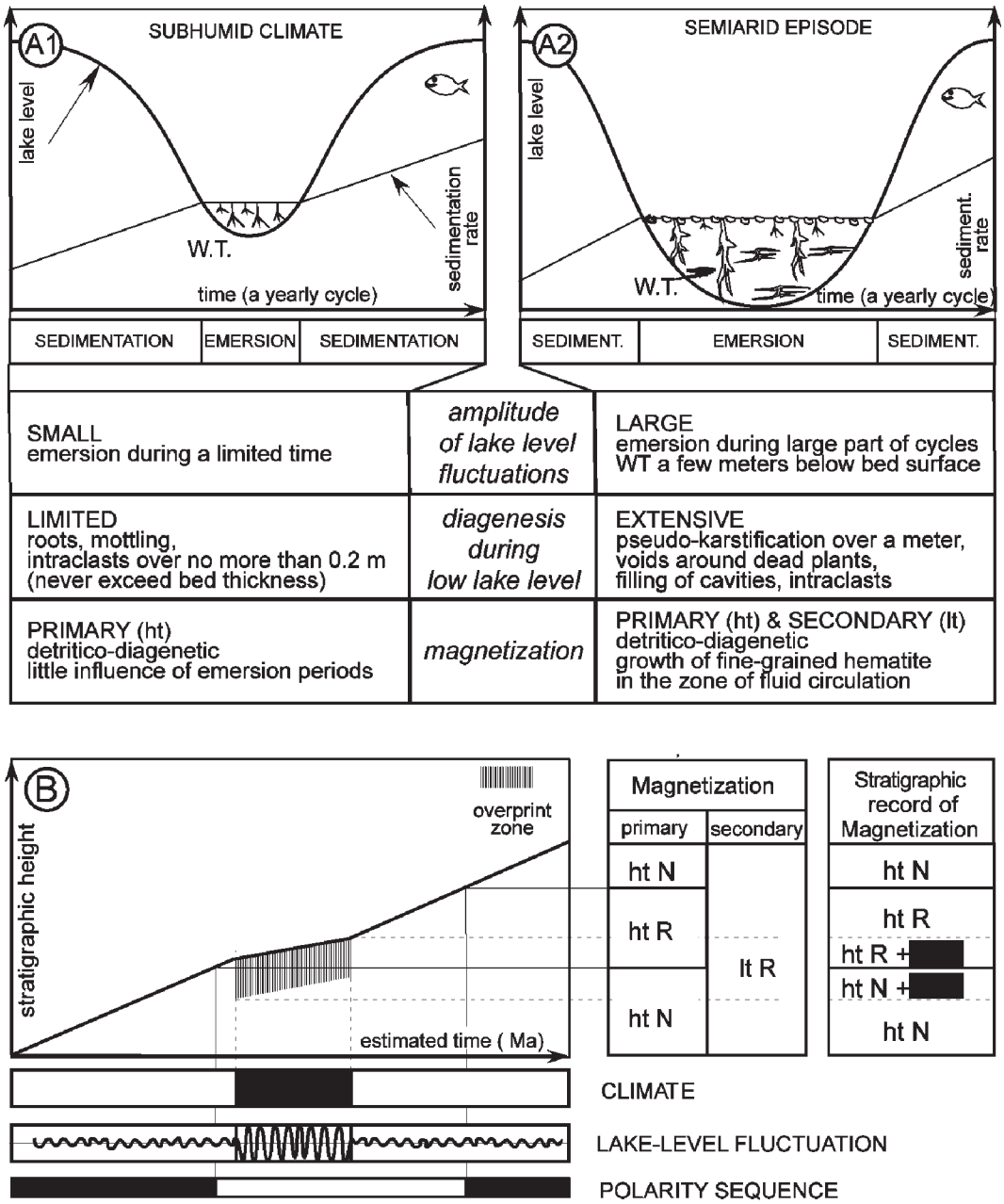

FIG. 13.—Schematic model of acquisition of the "lt magnetic component." **A)** Comparative evolution of a palustrine environment during subhumid climate (A1) and semiarid episode (A2). Sketch is drawn at the scale of an elementary cycle (yearly scale). **B)** Example of the acquisition of a complex magnetization. The ht magnetization is a primary detritico-chemical signal. The lt magnetization is interpreted as a diagenetic signal that was acquired during periods of large water-table fluctuations that enabled circulation of fluids of varied compositions and growth of magnetic minerals.

4 and 5. Limestones below and including the P. Galante Mbr correspond to a reversed-polarity interval. A possibly normal-polarity episode occurs within the first meters of the overlying siltstones. Overlying sediments show mineralogic transformations and are assigned to semiarid episode 4. The paleomagnetic signal of semiarid episode 4 is characterized by he result of remagnetization (as in VI section). The section ends with a normal-polarity interval. On the basis of correlations with ections in the western part of the basin, the P. Galante Mbr, the interval corresponding to semiarid episode 4 and the overlying sediments are assigned to chron 30R and to 29R–29N, respectively.

The Bréguières section is also well correlated in the field with the other sections. Outside of the samples taken from an active quarry (Galbrun 1997), data are sparse and highly overprinted. The N–R sequence (in quarry samples [60–72 m in BR section, Figs. 4, 14]) is correlated with the 31N–30R sequence.

Correlation with Global Climatic Fluctuations

The relatively precise chronostratigraphy of the studied interval in the Aix-en-Provence basin allows a comparison with other climatic data from the same period, especially with those documented from the paleoceanographic studies (Barrera and Savin 1999, Abreu et al. 1998).

The climate during semiarid episodes 1 and 2 probably did not differ significantly from the subhumid climate. Sediments deposited during the

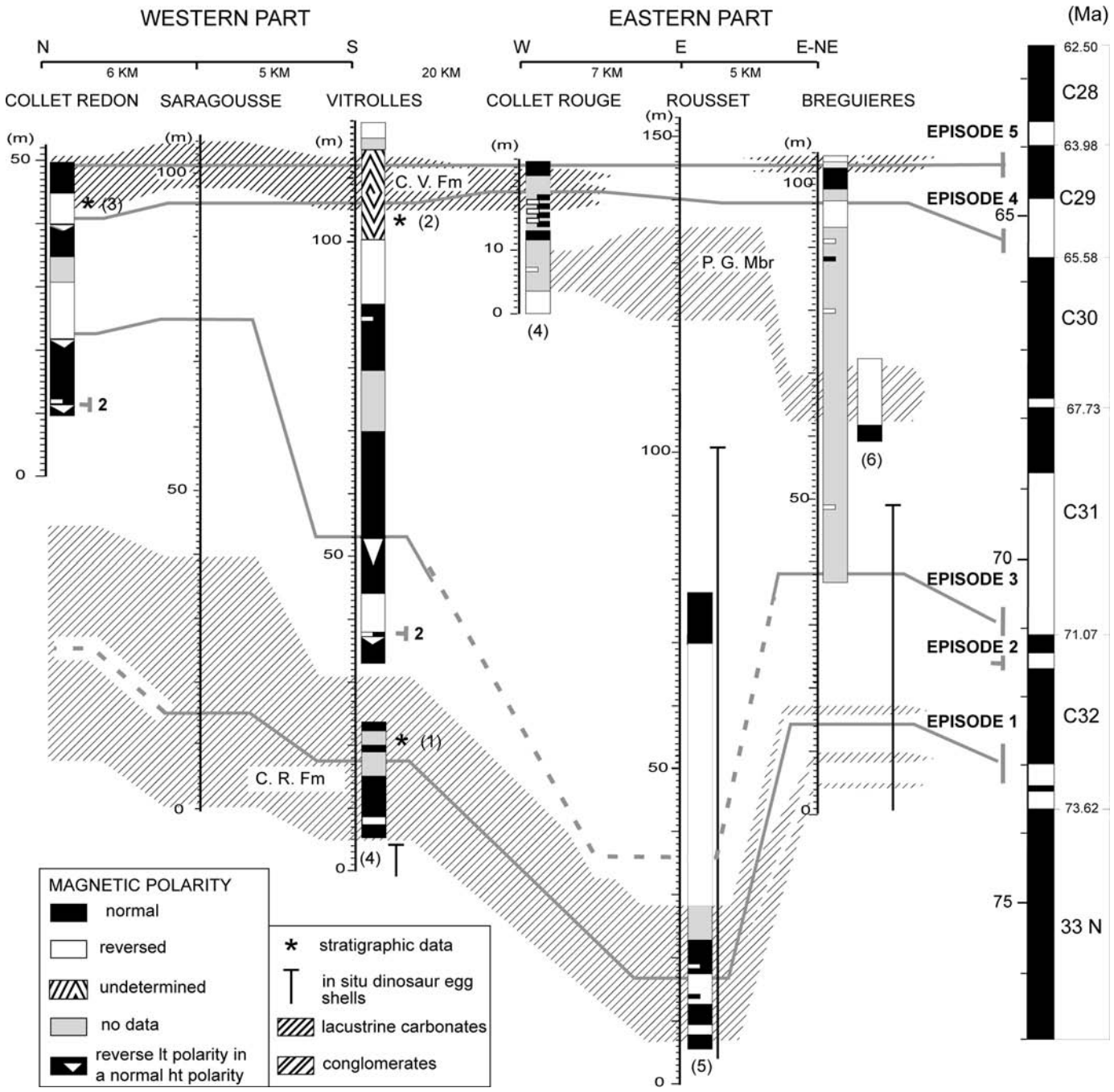

FIG. 14.—Magnetostratigraphy at the basin scale. The paleomagnetic data are presented according to stratigraphic height. The lithostratigraphic units are represented by shaded zones. The correlation lines correspond to the semiarid episodes and are tied to the standard paleomagnetic scale. Correlation line corresponding to semiarid episode 5 has been arbitrarily set to horizontal. Biostratigraphic data (1, Feist-Castel 1975; 2, Vasseur 1898), chemostratigraphy (3, Cojan et al. 2000), paleomagnetic data (4, Westphal and Durand 1990; 5, Krumsiek and Hahn 1989; 6, results from the quarry, Galbrun 1997; paleomagnetic data from 4 and 5 confirmed through the last normal polarity up to 76 m by Kissel, unpublished data).

semiarid episodes are characterized by emersion features or smectite-dominated clay assemblages, respectively. They were deposited at the end of the Campanian, a time characterized by a warm climate and a relatively high global sea level (Abreu et al. 1998; Barrera and Savin 1999). It should be noted that the C. Rognac Fm is composed of several shallowing-upward successions that reflect higher-frequency cycles.

Semiarid episode 3, pseudo-gley paleosols, and the P. Galante Fm occurred during a time interval characterized by a cooling trend interrupted by some high-frequency warm intervals (Barrera and Savin 1999). Semiarid episode 3 probably occurred during one of these high-frequency warm intervals, whereas the pseudo-gley paleosols and the P. Galante Mbr were deposited during cooler intervals during the Maastrichtian (Gomez-Alday et al. 2004). Wetter conditions allowed development of pseudo-gley soils instead of the carbonate-rich ones that formed under the semihumid conditions. Stream flows also increased and conglomerates were transported under these more humid conditions.

Semiarid episode 4 occurred during an interval of the global warmth and climatic instability that characterized the end of the Cretaceous. It has been suggested that an increase in temperature, estimated at around 6°C (Wilf et al. 2003), could have resulted from the main Deccan flood basalt event (dated between 67 and 64 Ma, Bhattacharji et al. 1996; Hofmann et al. 2000; Wignall 2001).

Semiarid episode 5 reflects warming that occurred at the beginning of the Paleocene (Abreu et al. 1998).

Although there is a good accordance between the climate variations characterized in the Provence basin and the large climatic trends defined in the Late Cretaceous–early Paleocene, we cannot propose a more precise correlation.

CONCLUSION

The primary result of this study is the correlation of the climate changes in the Provence basin to the global system. These changes recorded in a hydrologically closed continental basin correlate quite well with the global climate evolution.

Additional results are:

- semiarid episodes in the basin promoted mineralogic transformations that resulted in complex paleomagnetic signals due to diagenetic growth of magnetic minerals in association with water-table fluctuations. Climate changes promoted fluctuations in sediment supply to the basin.
- Correlations based on the identified semiarid episodes combined with paleomagnetic data permit correlation of the Provence successions with the GPTS (geomagnetic polarity time scale). These correlations indicate a strong diachronism of the lithostratigraphic units.
- Facies variability, including those recording the semiarid episodes, is closely linked to basin topography.

ACKNOWLEDGMENTS

G. Cheylan is thanked for his support during the field work. We are grateful to M. Pinault and E. Lorentz for their help during the sampling. The authors are grateful to the reviewers T. Demko, D. Elmore, G. Muttoni, and to Editor Colin North and Associate Editor Jacqueline Huntoon for their helpful comments.

REFERENCES

Abreu, V.S., Hardenbol, J., Haddad, G.A., Baum, G.R., Droxler, A.W., and Vail, P.R., 1998, Oxygen isotope synthesis: a Cretaceous ice-house?:, SEPM, Special Publication 60, p. 75–80.

Ashraf, A.R., and Erben, H.K., 1986, Palynologishe Untersuchung an der Kreide/Tertiär–Grenze West-Mediterraner Regionen: Paleontographica, v. 200, p. 11–163.

Babinot, J.F., and Durand, J.P., 1980a, Valdonien, Fuvélien, Bégudien, Rognacien, Vitrollien. Les étages français et leurs stratotypes: Orléans, France, Bureau de Recherche Géologique et Minière, Mémoires, v. 109, p. 92–171.

Babinot, J.F., and Durand, J.P., 1980b, Rognacien, Vitrollien. Les étages français et leurs stratotypes: Orléans, France, Bureau de Recherche Géologique et Minière, Mémoires, v. 109, p. 184–192.

Barrera, E., and Savin, S.M., 1999, Evolution of late Campanian–Maastrichtian marine climates and oceans, *in* Barrera, E., and Johnson, C.C., eds., Evolution of the Cretaceous Ocean–Climate System: Geological Society of America, Special Paper 332, p. 245–282.

Bhattacharji, S., Chatterjee, N., Wampler, J.M., Nayak, P.N., and Deshmukh, S.S., 1996, Indian interplate and continental rifting, lithospheric extension, and mantle upwelling in Deccan flood basalt volcanism near the K/T boundary: evidence from mafic dike swarms: Journal of Geology, v. 104, p. 379–398.

Besse, J., and Courtillot, V., 2002, Apparent and true polar wander and the geometry of the geomagnetic field over the last 200 Myr: Journal of Geophysical Research, v. 107-B11, 2300, DOI: 10.1029/2000JB000050.

Blair, T.C., and Bilodeau, W.L., 1988, Development of tectonic cyclothems in rift, pull-apart, and foreland basins: sedimentary response to episodic tectonism: Geology, v. 16, p. 517–520.

Cande, S.C., and Kent, D.V., 1995, Revised calibration of the geomagnetic polarity time scale for the Late Cretaceous and Cenozoic: Journal of Geophysical Research, v. 100, p. 6093–6095.

Carroll, A.R., and Bohacs, K.M., 1999, Stratigraphic classification of ancient lakes: balancing tectonic and climatic controls: Geology, v. 27, p. 99–102.

Cecil, C.B., 1990, Paleoclimatic controls on stratigraphic repetition of chemical and siliciclastic rocks: Geology, v. 18, p. 533–536.

Chorowitz, J., Mekarnia, A., and Rudant, J.-P., 1989, Inversion tectonique dans le massif de Sainte-Victoire (Provence, France). Apport de l'imagerie *Spot*: Paris, Académie des Sciences, Comptes Rendus, v. 308, p. 1179–1185.

Cojan, I., 1989, Discontinuités majeures en milieu continental. Proposition de corrélation avec évènements globaux (Bassin de Provence, S. France, passage K/T): Paris, Académie des Sciences, Comptes Rendus, v. 309, p. 1013–1018.

Cojan, I., 1993, Alternating fluvial and lacustrine sedimentation: Tectonic and climatic controls (Provence basin, S. France, Upper Cretaceous/Paleocene): International Association of Sedimentologists, Special Publication 17, p. 425–438.

Cojan, I., 1999, Carbonate-rich palaeosols in the Late Cretaceous–early Palaeogene series of the Provence Basin (France): International Association of Sedimentologists, Special Publication 27, p. 323–335.

Cojan, I., Moreau, M.-G., and Stott, L.E., 2000, Stable carbon isotope stratigraphy of the Paleogene pedogenic series of southern France as a basis for continental-marine correlation: Geology, v. 28, p. 259–262.

Colson, J., 1996, Découpage séquentiel de dépôts fluvio-lacsutres à paléosols carbonatés: interprétation climatique et hydrologique (Danien, bassin d'Aix-en-Provence, France): Paris, Ecole des Mines de Paris, Mémoires Sciences de la Terre, v. 26, 175 p.

Colson, J., and Cojan, I., 1996, Groundwater dolocretes in a lake marginal environment: an alternative model for dolocrete formation in continental settings (Danian of the Provence Basin, France): Sedimentology, v. 43, p. 175–188.

Colson, J., Cojan, I., and Thiry, M., 1998, A hydrological model for palygorskite formation in the Danian continental facies of the Provence Basin (France): Clay Minerals, v. 33, p. 337–347.

Dardeau, G., 1987, Tectonic inversion and permanence of the structural units during the Mesozoic and Alpine history of the French Maritime Alps basin, part of the former passive margin of Tethys: Paris, Académie des Sciences, Comptes Rendus, v. 305, p. 483–486.

De Celles, P.G., 1986, Sedimentation in a tectonically partitioned, nonmarine foreland basin: the Lower Cretaceous Kootenai Formation, southwestern Montana: Geological Society of America, Bulletin, v. 97, p. 911–931.

Dercourt, J., Gaetani, M., Vrierlynk, B., Barrier, E., Biju-Duval, B., Brunet, M.F., Cadet, J.P., Crasquin, S., and Sandulescu, M., eds., 2000, Atlas Peri-Tethys: 24 paleogeographical maps.

Diessel, C., Boyd, R., and Wadworth, J., 2000, On balanced and unbalanced accommodation/peat ratios in the Cretaceous coals from the Gates Formation, western Canada, and their sequence-stratigraphic significance: International Journal of Coal Geology, v. 43, p. 143–186.

Duchaufour, P., 2001, Introduction à la Science du Sol: Paris, Dunod, 331 p.

Durand, J.P., 1989, Le synclinal de l'Arc et la limite Crétacé–Paléocène: Digne, France, Cahiers de la Réserve Géologique de Haute-Provence, v. 1, p. 2–10.

Durand, J.P., and Guieu, G., 1980, Cadre structural du bassin de l'Arc. Le gisement de charbon du bassin de l'Arc (Houillères de Provence): Industrie Minérale, supplement 62, p. 3–12.

Feist-Castel, M., 1975, Répartition des Charophytes dans le Paléocène et l'Eocène du bassin d'Aix-en-Provence: Société Géologique de France, Bulletin, v. 17, p. 88–97.

Freytet, P., and Plaziat, J.C., 1982, Continental Carbonate Sedimentation and Pedogenesis; Late Cretaceous–early Tertiary of Southern France: Stuttgart, E. Schweizerbart'sche Verlagsbuchhandlung, Science Publishers, Contributions to Sedimentology 12, 213 p.

Galbrun, B., 1989, Résultats magnétostratigraphiques à la limite Rognacien–Vitrollien: precisions de la limite Crétacé–Tertiaire dans le basin d'Aix-en-Provence: Digne, France, Cahier de la Réserve Géologique de Haute-Provence, v. 1, p. 38–42.

Galbrun, B., 1997, Did the European dinosaurs disappear before the K/T event? magnetostratigraphic evidence: Earth and Planetary Science Letters, v. 148, p. 569–579.

Galbrun, B., Rasplus, L., and Durand, J.P., 1991, La limite Crétacé/Tertiaire dans le domaine provençal: étude magnétostratigraphique du passage Rognacien–Vitrollien à l'ouest du synclinal de l'Arc: Paris, Académie Sciences, Comptes Rendus, v. 312, p. 1467–1473.

Gaviglio, P., 1985, A fault and stress field analysis in a coal mine (Gardanne, Bouches-du-Rhône, France): Tectonophysics, v. 113, p. 349–366.

Gaviglio, P., 1987, Conséquences de l'évolution structurale sur les caractéristiques physiques des calcaires fuvéliens du Bassin de l'Arc (Bouches-du-Rhône, France): fracturation, propriétés mécaniques, états de contraintes: Géologie Méditerranéenne, v. 14, p. 221–232.

Glintzboeckel, C., 1980, Le gisement de charbon du basin de l'Arc (houillères de Provence), reconnaissance de l'extension du gisement: Paris, Industrie Minérale, suppl. 62, p. 41–53.

Gomez-Alday, J.J., Lopez, G., and Elorza, J., 2004, Evidence of climatic cooling at the Early/Late Maastrichtian boundary from Inoceramid distribution and isotopes: Sopelana sections, Basque Country, Spain: Cretaceous Research, v. 25, p. 649–668.

Heller, P.L., and Paola, C., 1992, The large-scale dynamics of grain-size variation in alluvial basins, 2: Application to syntectonic conglomerate: Basin Research, v. 4, p. 91–102.

HOFMANN, C., FERAUD, G., AND COURTILLOT, V., 2000, $^{40}Ar/^{39}Ar$ dating of mineral separates and whole rocks from the western Ghats lava pile: Further constraints on duration and age of Deccan taps: Earth and Planetary Science Letters, v. 180, p. 13–27.

HOPPIE, B., AND GARRISON, R.E., 2002, The Cuyama strike-slip basin, California, USA: an example of contracting syntectonic and post tectonic strata: Journal of Sedimentary Research, v. 72, p. 268–287.

KIRSCHVINK, J.L., 1980, The least-squares line and plane and the analysis of paleomagnetic data: Royal Astronomical Society, Geophysical Journal, n. 62, p. 699–718.

KRUMSIEK, K., AND HAHN, G.G., 1989, Magnetostratigraphy near the Cretaceous/Tertiary boundary at Aix-en-Provence (southern France): Digne, France, Cahier de la Réserve Géologique de Haute-Provence, v. 1, p. 38–42.

LACOMBE, O., ANGELIER, J., AND LAURENT, P., 1992, Determining paleostress orientations from faults and calcite twins: a case study near the Sainte-Victoire Range (southern France): Tectonophysics, v. 201, p. 141–156.

LEEDER, M.R., HARRIS, T., AND KIRKBY, M.J., 1998, Sediment supply and climate change; implications for basin stratigraphy: Basin Research, v. 10, p. 7–18.

LOWRIE, W., 1990, Identification of ferromagnetic minerals in a rock by coercivity and unblocking temperature properties: Geophysical Research Letters, v. 17, p. 159–162.

MARTINIUS, A.W., 2000, Labyrinth facies architecture of the Tortola fluvial system and controls on deposition (late Oligocene–early Miocene, Loranca basin, Spain: Journal of Sedimentary Research, v. 70, p. 850–867.

MAY, M.T., FURER, L.C., KVALE, E.T., SUTTNER, L.J., JOHNSON, G.D., AND MEYERS, J.H., 1995, Chronostratigraphy and tectonic significance of Lower Cretaceous conglomerates in the foreland of central Wyoming, *in* Dorobek, S.L., and Ross, G.M., eds., Stratigraphic Evolution of Foreland Basins: SEPM, Special Publication 52, p. 97–110.

MCFADDEN, P.L., AND MCELHINNY, M., 1988, The combined analysis of remagnetization circles and direct observation in paleomagnetism: Earth and Planetary Science Letters, v. 87, p. 161–172.

MCFADDEN, P.L., AND MCELHINNY, M., 1990, Classification of the reversal test in paleomagnetism: Geophysical Journal International, v. 103, p. 725–729.

MEDUS, J., 1972, Palynological zonation of the Upper Cretaceous in southern France and northeastern Spain: Revue de Paléobotanique et de Palynologie, v. 14, p. 287–295.

OLSEN, P.E., 1990, Tectonic, climatic, and biotic modulation of lacustrine ecosystems: examples from Newark Supergroup of eastern North America, *in* Katz, B.J., ed., Lacustrine Basin Exploration: Case Studies and Modern Analogs: American Association of Petroleum Geologists, Memoir 50, p. 209–224.

PAOLA, C., HELLER, P.L., AND ANGEVINE, C.L., 1992, The large-scale dynamics of grain-size variation in alluvial basins, 1: Theory: Basin Research, v. 4, p. 73–90.

PARIS, A., 1969, Relation entre la déformation et la fracturation des roches en Provence [Thèse 3ème cycle]: Université Grenoble, 116 p.

POSAMENTIER, H.W., AND ALLEN, G.P., 1993, Siliciclastic sequence stratigraphic patterns in foreland ramp-type basins: Geology, v. 21, p. 455–458.

ROUIRE, J., L'HOMER, A., BLANC, J.J., AND GAUBERT, J., 1979, Carte géologique France (1/250,000), feuille Marseille (39): Orléans, Bureau Recherches Géologiques et Minières, 88 p.

SMITH, G.A., 1994, Climatic influences on continental deposition during late-stage filling of an extensional basin, southeastern Arizona: Geological Society of America, Bulletin, v. 106, p. 1212–1228.

THIRY, M., FORETTE, N., AND SCHMITT, J.M., 1983, Technique de diffraction des rayons X et interprétation des diagrammes: Paris, Ecole des Mines de Paris, Note Technique, 51 p.

VASSEUR, G., 1898, Sur la découverte de fossiles dans les assises qui constituent en Provence la formation dite étage de Vitrolles, et sur la limite des terrains crétacés et tertiaires dans le bassin d'Aix (Bouches-du-Rhône): Paris, Académie des Sciences, Comptes Rendus, v. 127, p. 890–892.

WESTPHAL, M., AND DURAND, J.-P., 1990, Magnétostratigraphie des séries continentales fluvio-lacustres du Crétacé supérieur dans le synclinal de l'Arc (région d'Aix-en-Provence, France): Société Géologique de France, Bulletin, v. 8, p. 609–620.

WIGNALL, P.B., 2001, Large igneous provinces and mass extinctions: Earth-Science Reviews, v. 53, p. 1–33.

WILF, P., JOHNSON, K., AND HUBER, T., 2003, Correlated terrestrial and marine evidence for global climate changes before mass extinction at the Cretaceous–Paleogene boundary: National Academy of Sciences, Proceedings, v. 100, p. 599–604.

Received 5 November 2004; accepted 8 September 2005.